Global NEST Journal, Vol 20, No 2, pp 216-225

Inorganic carbon removal from refinery wastewater by using TiO_2/ZnO/Fenton photocatalyst

Aljuboury D.A.D.A.* and Palaniandy P.
School of Civil Engineering, Universiti Sains Malaysia, Nibong Tebal, Seberang Perai Selatan, Pulau Pinang, 14300, Malaysia.
Received: 05/06/2017, Accepted: 02/01/2018, Available online: 02/05/2018
*to whom all correspondence should be addressed: e-mail: msc.dheeaa@yahoo.com

Abstract

The aim of this study is to investigate the performance of the solar photocatalyst of TiO_2/ZnO/Fenton process to treat the refinery wastewater and remove inorganic carbon (IC) which potentially toxic to human, aquatic and microorganism life. Central composite design with response surface methodology was used to evaluate the relationships between operating variables for TiO_2 dosage, ZnO dosage, Fe^{2+} dosage, H_2O_2 dosage, and pH to identify the optimum operating conditions. Quadratic models for inorganic carbon (IC) removal and residual iron prove to be significant with low probabilities (<0.0001). The (IC) removal rates and residual iron correspond well with the predicted models. The maximum removal rate for IC and residual iron was 92.3% and 0.013, respectively at optimum operational conditions of a TiO_2 dosage (0.3 g/l), ZnO dosage (0.58 g/l), Fe^{2+} dosage (0.02 g/l), H_2O_2 dosage (2.7 g/l), and pH (7). The treatment process achieved higher degradation efficiencies for IC and reduced the treatment time comparing with other related processes.

Keywords: Advanced oxidation process (AOP); Petroleum wastewater; Inorganic carbon (IC); Response surface methodology (RSM); Solar photo-catalyst of TiO_2/ZnO/Fenton process

1. Introduction

The environmental dangers due to chemical pollution in the water have become increasingly serious and directly related to industrial development. The contamination of water by carbon compounds has been recognized as an issue of growing importance in recent years. The presence of inorganic carbon compounds in wastewater such as carbonyl sulfide, polyatomic ions and carbonate is potentially toxic to human, aquatic and microorganism life. Carbon compounds is considerable health concern, even at low concentration and is well known human carcinogen.

Advanced oxidation processes (AOPs) have the capability of rapid degradation of recalcitrant pollutants in the aquatic environment (Gogate and Pandit 2004; De Morais and Zamora, 2005). Depending on the techniques used the AOP processes can be divided into two groups; Abiotic degradation, (e.g. thermal degradation (combustion), molten salt processes, wet oxidation, chemical oxidation, acid-base hydrolysis) and photo-degradation, (e.g. TiO_2/H_2O_2/UV, O_3/UV or O_3/H_2O_2/UV processes, solar photolysis, processes in vacuum ultraviolet and photocatalysis) (Sobczyński and Dobosz, 2001). Remediation of hazardous substances is attributed to hydroxyl radical (•OH), which exhibits reactivity toward organics (Kim *et al.,* 2012; Aljuboury *et al.,* 2015a), which has a high oxidation potential (estimated to be 2.8 V) relative to other oxidants (Al-Rasheed, 2005). The generation of hydroxyl and superoxide radicals was more in the TiO_2 exposed to UV condition as compared to the TiO_2 exposed to visible light and dark condition (Mathur *et al.,* 2015).

Several techniques to enhance the production rate of hydroxyl radical (•OH) by catalysts (such as zinc oxide (ZnO) and titanium oxide (TiO_2)), chemical additives (such as H_2O_2), external energy (such as UV and sunlight), and the integration of two or more AOPs (such as ZnO/Fenton/sunlight) has been reported (Kim *et al.,* 2012). The photo-degradation efficiency of carbon compounds is found to be dependent on nature and the concentration of carbon compounds and the amount of photo-catalyst (Barick *et al.,* 2015).

Several previous studies have reported the enhanced oxidation of contaminants by the integration of two or more AOPs (such as ZnO/TiO_2, ZnO/Fenton/sunlight and TiO_2/Fenton). Al Jabri and Feroz (2015) reported that the removal efficiency of inorganic carbon for the combination of ZnO/TiO_2 process was 26% at 180 min in aqueous solutions. Tony *et al.,* 2009 reported that an 84% COD removal in the diesel oil-water emulsion was achieved by using Fenton/TiO_2/UV while the using Fenton/ZnO/UV under same conditions resulted in a reduction of about 18% in the COD removal efficiency. This result may be because the surface area of TiO_2 is more than that for ZnO.

The most common design under response surface methodology (RSM) is central composite design (CCD) which is efficient and flexible, providing sufficient data on the effects of variables and overall experiment error with a minimum number of experiments (Ahmad *et al.,* 2005).

In this study, the combined photo-catalytic TiO_2 and ZnO with Fenton process were used for petroleum wastewater treatment. The aims of this study were as follows:

- To investigate the performance of solar photocatalyst of TiO_2/ZnO/Fenton process in petroleum wastewater treatment.
- To evaluate the performance of employing this process by a CCD with RSM to degradation of IC from the petroleum wastewater.
- To evaluate the statistical relationships among operating variables (such as TiO_2 dosage, ZnO dosage, Fe^{+2} dosage, H_2O_2 dosage, and pH) and the responses, which IC removal efficiencies and residual iron were selected as the responses for optimization.
- To determine the optimum operational conditions of the proposed method.
- To compare the proposed method with the previous works.

2. Materials and methods

2.1. Sampling and characterization

Samples of the petroleum wastewater were collected from SOR, Oman. Samples were transferred to the laboratory and stored under refrigeration (4 °C) until use. Samples were characterized before the experiments to obtain their chemical and physical properties. The petroleum wastewater characterization was determined by the quantification of pH, IC according to the Standard Methods for the Examination of Wastewater methodology. General characteristics of the petroleum wastewater are summarized in Tables 1.

Table 1. Characteristics of petroleum wastewater from SOR

No	Parameter	Range of concentrations in petroleum wastewater	Average	The standard discharge limit*
1	pH	6-8	7	6 < pH > 9
2	Conductivity (uS/cm)	2600-3950	3275	< 2700
3	TDS (ppm)	1200-1500	1350	< 2000
4	TOC (ppm)	220 - 265	243	< 50
5	IC (ppm)	45-59	52	< 10
6	D.O. (ppm)	0.6-2.9	1.75	> 5
7	Phenol (ppm)	70-90	80	0.001
8	Oil (ppm)	15-22	19	0.001
9	Iron (ppm)	<0.01	<0.01	2
10	Sulfite(ppm)	12-15	13.5	1.0

2.2. Experimental procedure

In the current study, the powder of ZnO and TiO_2 Aeroxide P-25 (manufactured by Evonik Industries Co., Germany) were used for photo-catalytic oxidation of petroleum wastewater. A schematic diagram of solar photo-catalyst TiO_2/ZnO/Fenton process is shown in Figure 1. It consisted of a glass recirculation tank (1.5 L), which was subjected to stirring to maintain a well-mixed solution during the experiments, connected to the tubular solar reactor (four tubes of 50 cm length × 2 cm inner diameter × 0.1 cm thickness). The solution was recirculated through the reactor at a flow rate of about 1.5 L/min using a peristaltic pump. The chemical materials were added in a glass recirculation tank in this process. The pH for petroleum wastewater samples was adjusted between 3 and 7 during the experiments. The tubular photo reactor was operated under exposure category of very high (8-11) according to a UV-index.

As shown in Table 2, each independent variable was varied over three levels according to face-centered CCD as -1, 0, and 1, respectively, at the determined ranges base on a set of preliminary experiments. The total number of experiments conducted for the five factors according to Equation (1) (Mohajeri *et al.,* 2010a; El-Gendy *et al.,* 2013).

$$\text{No: of experiments} = 2^k + 2k + 8 \quad (1)$$

Where:

k was the number of factors.

The design consisted of 2^k factorial points augmented by 2k axial points and eight replications for a center point. In this work, the total number of experiments conducted for the five factors was 50 with 32 factorial points, ten axial points and eight replications to assess the pure error and got a good estimate. The behavior of the system was explained through an empirical second-order polynomial model, as shown in Equation (2) (Montgomery 2008):

$$Y=\beta_0+\sum_{j=1}^{k}\beta_j X_j+\sum_{j=1}^{k}\beta_{jj} X_j^2+\sum_{i}\sum_{<j=2}^{k}\beta_{ij} X_i X_j+e_j \quad (2)$$

Where:

Y is the response.

X_i and X_j are the variables.

β is the regression coefficient.

k is the number of factors studied and optimize in the experiment.

e_i is the random error.

Table 2. Central composite design (CCD) independent variables

The actual factors	The coded factors	Level of value		
		Low level (-1)	Center (0)	High level (+1)
TiO_2 (g L^{-1})	A	0.3	0.5	0.7
ZnO (g L^{-1})	B	0.3	0.5	0.7
Fe^{+2} (g L^{-1})	C	0.01	0.11	0.2
H_2O_2 (g L^{-1})	D	0.5	2.25	4.0
pH	E	3	5	7

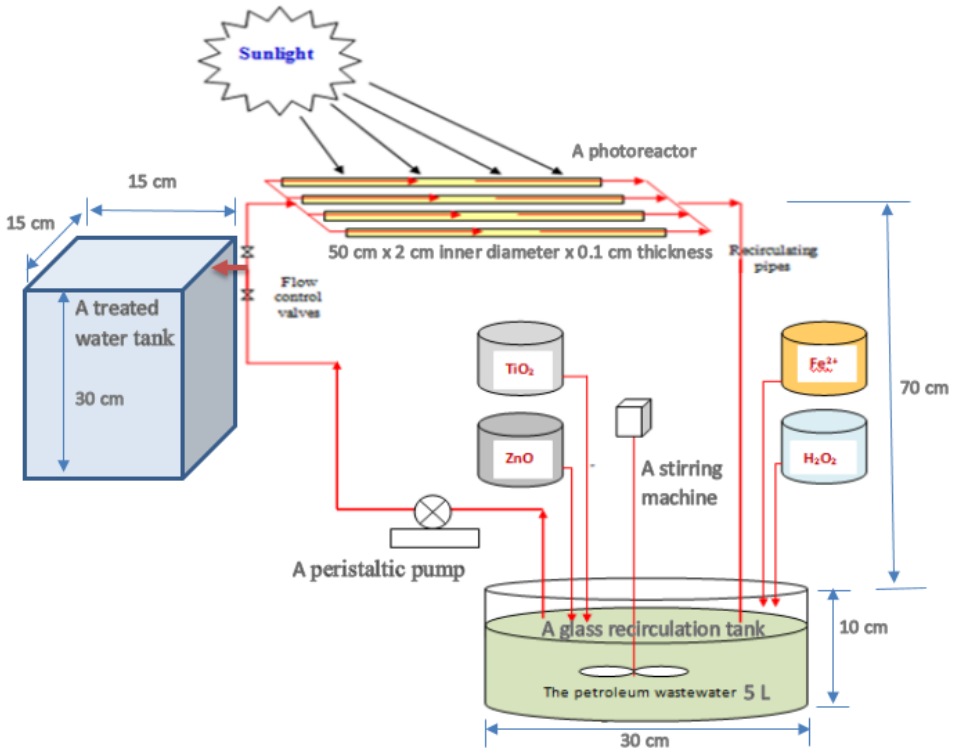

Figure 1. Schematic diagram of solar photo-catalyst of TiO_2/ZnO/Fenton process

Several sets of experiments were carried out to evaluate the effectiveness of this process to treat the petroleum wastewater and investigate the influence of important operating parameters, including catalysts dosage and pH on removal efficiencies of IC. The UV-index is calculated as follows.

Solar UV radiation was measured by a global UV radiometer (KIPP & ZONEN, ISO 17166:1999/CIE S007/E-1998). The UV-index is calculated as follows.

Take the output from the UV-E radiometer according to ISO 17166:1999/CIE S007/E-1998. Transform the output voltage (v/m) to W/m^2 with the instruments sensitivity (40 m^2/W):

$$R\left(\frac{w}{m^2}\right) = 0.168\ R\left(\frac{v}{m}\right) \quad (3)$$

$$UVI = R\left(\frac{w}{m^2}\right) * 40\left(\frac{m^2}{w}\right) \quad (4)$$

Where:

UVI is the UV-index;

R is the reading (R) in UV radiometer by (W/m^2) unit.

CCD and RSM were employed in the statistical design of the experiments. Data analysis, explaining the optimal conditions of the independent variables and assessment of the relationships among five significant independent variables, which were TiO_2 dosage, ZnO dosage, Fe^{+2} dosage, H_2O_2 dosage, and pH as shown in Tables 3 and 4 (Montgomery 2008).

Based on the IC values, the photo-catalytic degradation efficiency is calculated by using Equation (5):

$$X = \frac{(IC)0-(IC)t}{(IC)0} \quad (5)$$

Where:

X is photo-catalytic degradation of IC.

$(IC)_0$ and $(IC)_t$ stand for the initial and after any irradiation time, IC values.

Table 3. Responses values for different experiment conditions for the solar photo-catalyst of TiO_2/ZnO/Fenton process.

Run	Factors					Responses			
	TiO_2 (g L^{-1})	ZnO (g L^{-1})	Fe^{+2} (g L^{-1})	H_2O_2 (g L^{-1})	pH	IC removal			Residual iron (ppm)
						Initial IC (ppm)	Final IC (ppm)	IC removal (%)	
1	0.3	0.7	0.2	0.5	7	55	22	60	6.5
2	0.7	0.3	0.2	4	3	55	17.6	68	8.5
3	0.7	0.3	0.01	0.5	3	55	20.4	63	4.5
4	0.5	0.5	0.1	0.5	5	55	20.4	63	9.5
5	0.7	0.3	0.2	4	7	55	9.35	83	0
6	0.3	0.7	0.2	4	7	55	6.6	88	2.5
7	0.7	0.3	0.01	4	3	55	14.9	73	2
8	0.7	0.3	0.2	0.5	7	55	13.2	76	4
9	0.7	0.5	0.1	2.25	5	55	6	89	2
10	0.7	0.7	0.01	0.5	3	55	13.8	75	9
11	0.5	0.3	0.1	2.25	5	55	21.5	61	3.5
12	0.5	0.5	0.1	2.25	5	55	29.7	46	6
13	0.5	0.5	0.1	2.25	5	55	23	58	4.5
14	0.3	0.7	0.2	4	3	55	3.3	94	1.5
15	0.3	0.3	0.01	0.5	7	55	13.8	75	2.7
16	0.7	0.7	0.2	4	3	55	22.5	59	4
17	0.5	0.5	0.01	2.25	5	55	20.3	63	3
18	0.3	0.5	0.1	2.25	5	55	13.2	76	2.5
19	0.7	0.3	0.01	4	7	55	18	67.35	3.4
20	0.3	0.3	0.2	0.5	7	55	19.3	65	6
21	0.5	0.5	0.1	2.25	3	55	18.7	66	6.5
22	0.5	0.5	0.1	2.25	5	55	21.4	61	3
23	0.3	0.7	0.01	4	7	55	17.6	68	3.5
24	0.5	0.5	0.2	2.25	5	55	21	62	9
25	0.7	0.7	0.01	0.5	7	55	19.8	64	11
26	0.7	0.3	0.01	0.5	7	55	20.4	63	3.5
27	0.5	0.5	0.1	2.25	5	55	17.9	67.5	3.62
28	0.3	0.7	0.01	0.5	7	55	22.6	59	6.5
29	0.3	0.7	0.01	4	3	55	18.7	66	4
30	0.3	0.7	0.2	0.5	3	55	23.7	57	3.5
31	0.3	0.7	0.01	0.5	3	55	18.7	66	3.5
32	0.3	0.3	0.01	4	3	55	14.3	74	5
33	0.7	0.7	0.2	4	7	55	18.2	67	3.55
34	0.5	0.7	0.1	2.25	5	55	24.8	55	10
35	0.3	0.3	0.2	0.5	3	55	17.9	67.4	3.52
36	0.5	0.5	0.1	2.25	5	55	7.7	86	0
37	0.7	0.7	0.01	4	3	55	17.6	68	4
38	0.7	0.7	0.2	0.5	7	55	11	80	3
39	0.3	0.3	0.2	4	7	55	16	71	2.5
40	0.5	0.5	0.1	2.25	7	55	13.8	75	4.5
41	0.5	0.5	0.1	2.25	5	55	17	69	3.5
42	0.5	0.5	0.1	4	5	55	11.6	79	9
43	0.3	0.3	0.01	4	7	55	18.7	66	3.6
44	0.3	0.3	0.2	4	3	55	17.6	68	5
45	0.7	0.7	0.2	0.5	3	55	28.6	48	5.5
46	0.3	0.3	0.01	0.5	3	55	17.9	67.5	3.52
47	0.7	0.7	0.01	4	7	55	13.2	76	10
48	0.5	0.5	0.1	2.25	5	55	14.8	73	6.5
49	0.7	0.3	0.2	0.5	3	55	15.4	72	11
50	0.5	0.5	0.1	2.25	5	55	23.1	58	4

Table 4. ANOVA results and adequacy of the quadratic models for IC removal efficiency and residual iron (RI)

	Source	S.S.	DF	MS	F-Value	Prob > F
IC	Model	4472.57	16	279.54	52.01	< 0.0001
	A	1.88	1	1.88	0.35	0.558
	B	8.5	1	8.5	1.58	0.2174
	C	474.38	1	474.38	88.26	< 0.0001
	D	98.94	1	98.94	18.41	0.0001
	E	0.029	1	0.029	5.47E-03	0.9415
	A^2	105.77	1	105.77	19.68	< 0.0001
	B^2	793.06	1	793.06	147.56	< 0.0001
	E^2	2185.78	1	2185.78	406.69	< 0.0001
	AB	318.78	1	318.78	59.31	< 0.0001
	AD	52.53	1	52.53	9.77	0.0037
	AE	225.78	1	225.78	42.01	< 0.0001
	BC	26.28	1	26.28	4.89	0.0341
	BD	22.78	1	22.78	4.24	0.0475
	CD	94.53	1	94.53	17.59	0.0002
	CE	57.78	1	57.78	10.75	0.0025
	DE	750.78	1	750.78	139.69	< 0.0001
	Residual	177.36	33	5.37		
	Lack of Fit	173.68	26	6.68	12.69	0.001
	Pure Error	3.68	7	0.53		
	Cor Total	4649.93	49			
RI	Model	356.4	17	20.96	161.88	< 0.0001
	A	3.43	1	3.43	26.49	< 0.0001
	B	4.03	1	4.03	31.09	< 0.0001
	C	3.69	1	3.69	28.49	< 0.0001
	D	4.1	1	4.1	31.62	< 0.0001
	E	4.82	1	4.82	37.21	< 0.0001
	B^2	17.68	1	17.68	136.48	< 0.0001
	C^2	1.5	1	1.5	11.58	0.0018
	E^2	4.75	1	4.75	36.71	< 0.0001
	AB	16.25	1	16.25	125.44	< 0.0001
	AC	4.35	1	4.35	33.6	< 0.0001
	AD	25.92	1	25.92	200.15	< 0.0001
	AE	44.65	1	44.65	344.79	< 0.0001
	BC	11.04	1	11.04	85.29	< 0.0001
	BD	154	1	154	1189.16	< 0.0001
	CD	8.82	1	8.82	68.11	< 0.0001
	CE	3.25	1	3.25	25.11	< 0.0001
	DE	19.22	1	19.22	148.41	< 0.0001
	Residual	4.14	32	0.13		
	Lack of Fit	4.11	25	0.16	35.77	< 0.0001
	Pure Error	0.032	7	4.60E-03		
	Cor Total	360.55	49			

2.3 Analytical study

A Shimadzu TC analyzer (LCSH/CSN) was used to measure the IC for each sample. IC was tested before and after treatment. Before each analysis, samples were filtered by filter papers (0.22 µm Millipore Durapore membrane, 40 Ashless, diameter 150 mm) to separate the solid catalyst.

3. Results and discussion

3.1. Experimental design and the analysis of variance

The analysis of variance (ANOVA) was used for graphical analysis of data to obtain the interaction between the process variables and the responses. The quality of the fit polynomial model was expressed by coefficient of determination (R^2). Model terms were evaluated by the P-value (probability) with 95% confidence level. All of the response surface quadratic models for parameters in Table 4 were significant at the 5% confidence level since the P-values were less than 0.05. The coefficients of determination (R^2) for the IC removal rate and residual iron

(RI) were 0.962 and 0.988 respectively, which were greater than 0.80, the cut-off for a model with good fit.

A high coefficient (R^2) value ensured a satisfactory adjustment of the quadratic model to the experimental data and illustrated good agreement between the calculated and observed results and showed that a desirable and reasonable agreement with the adjusted R^2 (Abu Amr *et al.,* 2013).

If the model terms had the P-value (probability) more than 0.05, they were considered limited influence. So, they must be excluded from the study to improve the models. The models of IC removal and RI were considered significant using the F-test at 5% significant level (Prob <0.05).

If the adequate precision (AP) ratio values are higher than 4, they are considered desirable and confirm that the predicted models could be used to navigate the space defined by the CCD (Noordin *et al.,* 2004). So, the 'AP' ratio values of the models in this study were considered adequate because they were 32.94 and 51.38 (higher than 4).

Empirical relationships among the variables and IC removal efficiency after excluding insignificant coefficients were presented by the following polynomial Equations (6) and (7):

$$\text{IC Removal}=65.12- 0.24A +0.5B -3.74C -1.71D -0.03E -6A^2 -16.5B^2 +27.5E^2 +3.2AB -1.3AD -2.7AE -0.9BC -0.8BD -1.7CD -1.3CE +4.8DE \quad (6)$$

$$\text{Residual iron}=3.52 -0.3A -0.3B +0.33C +0.4D +0.4E +2.5B^2 +0.72C^2 -1.28E^2 +0.7AB -0.37AC +0.9AD +1.18AE +0.59BC +2.19BD +0.52CD -0.3CE -0.8DE \quad (7)$$

Where:

A, B, C, D and E were model terms that represent coded factors TiO_2 dosage, ZnO dosage, Fe^{+2} dosage, H_2O_2 dosage, and pH, respectively.

Final equations in terms of actual factors were presented by the following Equations (8) and (9):

$$\text{IC Removal}= 104.5 +151.8TiO_2 +387ZnO +43.2Fe^{+2} -3.8H_2O_2 -67.7pH -151(TiO_2)^2 -413.5(ZnO)^2 +6.9(pH)^2 +79TiO_2ZnO -3.6TiO_2H_2O_2 -6.6TiO_2pH -47.7ZnOFe^{+2} -2.4ZnOH_2O_2 -10.3Fe^{+2}H_2O_2 -7Fe^{+2}pH +1.4H_2O_2pH \quad (8)$$

$$\text{Residual iron} =31.5 -29TiO_2 -89.7ZnO -17.7Fe^{+2} -3.5H_2O_2 +2.6pH +61.7(ZnO)^2 +79.7(Fe^{+2})^2 -0.3(pH)^2 +17.8TiO_2ZnO -19.4TiO2Fe^{+2} +2.6TiO_2H_2O_2 +2.9TiO_2pH +30.9ZnOFe^{+2} +6.3ZnOH_2O_2 +3.2Fe^{+2}H_2O_2 -1.7Fe^{+2}pH -0.2H_2O_2pH \quad (9)$$

The effects of the model terms on the IC removal efficiencies and Residual iron (RI) could be easily seen from Equations (17) and (18).

As can be seen in these equations, the first order effects of TiO_2 dosage, ZnO dosage, Fe^{+2} dosage, H_2O_2 dosage, and pH and second-order effects of TiO_2 dosage (A^2) and ZnO dosage (B^2), and second-order effect of pH (E^2) as well as the interaction (AB), (AD), (AE), (BC), (BD), (CD), (CE), and (DE) produced the main effect on the IC removal efficiency while for the residual iron (RI), the first order effects of TiO_2 dosage, ZnO dosage, Fe^{+2} dosage, H_2O_2 dosage, and pH and second-order effects of ZnO dosage (B^2) and Fe^{+2} dosage (C^2), and second-order effect of pH (E^2) as well as the interaction (AB), (AC), (AD), (AE), (BC), (BD), (CD), (CE), and (DE) produced the main effect on the residual iron (RI).

3.2. Three-dimensional plots of the regression and optimization process

Design Expert 6.0.7 was used to determine optimization of removal efficiency for IC. As shown in Figure 2, the response surfaces plots were created by Design Expert 6.0.7 and provided a three-dimensional view of the IC removal efficiencies and Residual iron (RI) surface over the independent variables. The main factors of this process that improved the IC removal efficiencies were TiO_2 dosage and ZnO dosage.

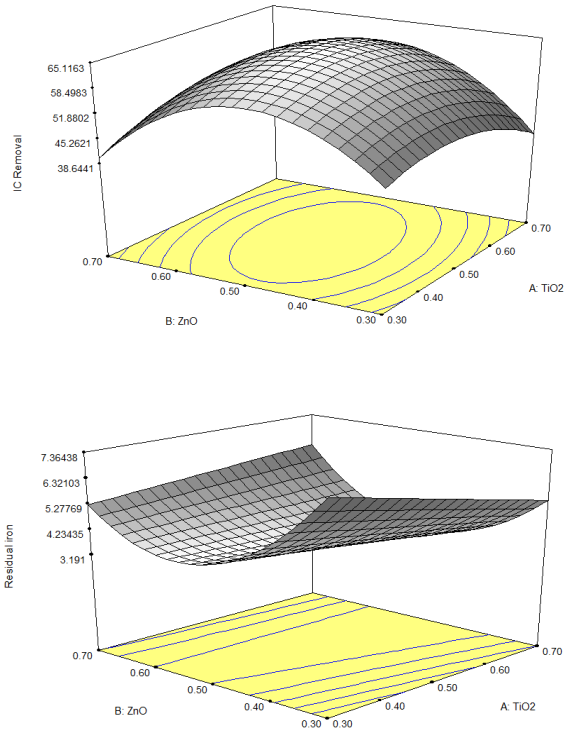

Figure 2. Response surface models for IC removal efficiencies and residual iron (RI) by the solar photo-catalyst of TiO_2/ZnO/Fenton process

According to the optimization step in the software Design Expert 6.0.7, the desired goals for the operational conditions (i.e., TiO_2 dosage, ZnO dosage, and pH) were chosen as "within" the range while (H_2O_2 and Fe^{2+} dosage) were chosen as "within" the minimum range to reduce the treatment cost.

The response (IC removal) were defined as "maximum" to achieve the highest performance while the residual iron response was defined as "within" the minimum range to evaluate the optimum amount of Fenton consumed for the optimal removal of IC.

The program combined individual desirability into a single number and then search to optimize this function based on the response goal. The model under optimized operational conditions predicted the IC removal rate was approximately 92.3, and the desirability function was 0.912. To confirm these results, an additional experiment under optimized operational conditions was carried out which revealed agreement with the predicted responses as shown in Table 5.

Table 5. Optimization results for maximum IC removal efficiency and minimum residual iron (RI) by the solar photocatalyst of TiO_2/ZnO/Fenton process

	TiO_2 (g L^{-1})	ZnO (g L^{-1})	H_2O_2 (g L^{-1})	Fe^{+2} (g L^{-1})	pH	IC (%)	(RI) (ppm)	Desirability
Selected solution	0.3	0.58	0.02	2.7	7	92.3	0.013	0.912
Lab experiments	0.3	0.58	0.02	2.7	7	90.5	0.015	-

The results of this search were compared with those of other works that treated the wastewater by approximately the same methods, for example, Al Jabri and Feroz (2015) reported that using the combination of ZnO/TiO_2 process to remove inorganic carbon (IC) achieved 26% of removal efficiency at 180 min in aqueous solutions. However, this method (the solar photocatalyst of TiO_2/ZnO/Fenton process) revealed that it was well efficient in petroleum wastewater treatment, achieving the highest removal rates for IC 90.5% at pH 7 and more economic by free energy (solar energy).

3.3. Effect of reaction time

It was found from the experiments that the photocatalytic reactions increase the inorganic carbon (IC) removal value with time as illustrated in Figure (3).

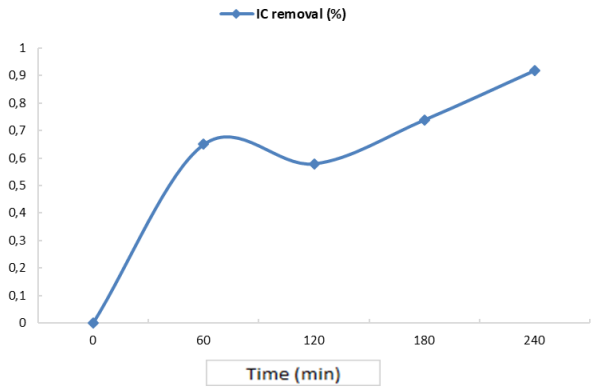

Figure 3. Variation in degradation rate of inorganics carbon (IC) during the solar photo-catalyst of TiO_2/ZnO/Fenton process at pH 7

However, sometimes decrease the inorganic carbon (IC) removal. The possible reasons might be the photocatalytic reactions oxidize pollutants and produce CO_2, which is considered inorganic. It can be seen from Figure (3) that inorganics are produced and consumed. This process achieved higher degradation efficiencies for IC and reduced the treatment time comparing with different processes under pH 7 as shown in Figure (4).

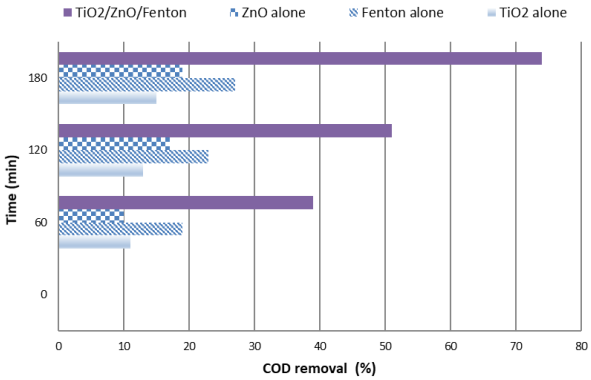

Figure 4. Comparing treatment time of the solar photocatalyst TiO_2/ZnO/Fenton process with different processes under pH 7.

3.4. Effect of TiO_2 and ZnO dosage

In the solar photocatalyst of TiO_2/ZnO/Fenton process, the TiO_2 and ZnO are two major chemicals that determine the operational efficacy as well as the costs. In order to maximize the effectiveness of the process, it is important to determine the optimal TiO_2/ZnO ratio. The optimization of catalyst concentration is key factor in achieving a satisfactory design (Akpan and Hameed, 2009). In TiO_2/ZnO oxidation, the reaction is activated by absorption of a photon with sufficient energy (equal or higher than the band-gap energy of the catalyst). The absorption leads to a charge separation due to promotion of an electron (e^-) from the valence band of the semiconductor catalyst such as TiO_2 or ZnO to the conduction band, thus generating a hole (h) in the valence band (Gaya and Abdullah, 2008; Eydivand and Nikazar, 2015). The relevant reactions at the semiconductor surface (such as TiO_2) governing the degradation of pollutants can be expressed as the following

equations (Konstantinou and Albanis, 2004; Eydivand and Nikazar, 2015):

$$TiO_2 + h\nu(UV) \rightarrow TiO_2(e^-_{CB} + h^+_{VB}) \quad (10)$$

$$TiO_2(h^+_{VB}) + H_2O \rightarrow TiO_2 + H^+ + \cdot OH \quad (11)$$

$$TiO_2(h^+_{VB}) + OH^- \rightarrow TiO_2 + \cdot OH \quad (12)$$

$$TiO_2(e^-_{CB}) + O_2 \rightarrow TiO_2 + \cdot O_2^- \quad (13)$$

$$\cdot O_2^- + H^+ \rightarrow HO_2\cdot \quad (14)$$

$$M + \cdot OH \rightarrow \text{degradation products} \quad (15)$$

$$M + h^+_{VB} \rightarrow \text{oxidation products} \quad (16)$$

$$M + e^-_{CB} \rightarrow \text{reduction products} \quad (17)$$

Where:

M: is the molecule of the pollutant

hv: is the photon energy required to excite the semiconductor electron from the valence band (VB) region to conduction band (CB) region

The oxidation occurs when a reactant loses electrons during the reaction while reduction occurs when a reactant gains electron during the reaction. When combined TiO_2 and ZnO, charge transfer can be enhanced, and the production of hydroxyl radical is also increased. Cheng *et al.,* (2014) monitored charge transfer from ZnO to TiO_2. In addition, Tony *et al.,* (2009) reported that the presence of TiO_2 is not only essential for the hydroxyl radicals (•OH) production, but also for the adsorption of the oil molecules on the TiO_2 surface.

Consequently, particular attention must be paid to TiO_2 and ZnO dosages in order to avoid the increase of turbidity in the petroleum wastewater during the solar photocatalyst of TiO_2/ZnO/Fenton process, which hinders the absorption of the sunlight required for this process, occurring in the presence of an excess of each of the two catalysts. The maximum removal efficiency of IC was 58% at a TiO_2/ZnO ratio of 0.52 and a TiO_2 dosage of 0.3. This behavior is in agreement with the findings by Al Jabri and Feroz, (2015) reported that the removal efficiency of inorganic carbon for the combination of ZnO/TiO_2 process was 26% at 180 min in aqueous solutions.

Various reasons for this behavior have been offered without much conviction or quantification. A possible explanation is that increased turbidity of the solution reduced the light transmission through the solution, while below this level of concentration, it was assumed that the catalyst surface and the absorption of light by TiO_2 particles were limiting (Mehrotra *et al.,* 2003; Heredia *et al.,* 2001).

Another case may be that of a near total light extinction which occurred by catalyst particles at an optimum concentration (Bickley *et al.,* 2005; Ahmed *et al.,* 2010; Adesina *et al.,* 2004). It seems that excess of each of the two catalysts has reverse effect by increase of turbidity in the wastewater and hinders the absorption of the sunlight. However, many authors have observed a reverse effect occur when the TiO_2 concentration increased to higher than the optimum value, the degradation rate declined due to the blocking of light penetration or the scattering and the interference of the light by the suspension. This, in turn, resulted in a reduction of the available active sites on the photocatalyst surface (Alhakimi *et al.,* 2003; Chakrabarti and Dutta, 2004; Gaya and Abdullah, 2008; Ehrampoush *et al.,* 2011; Eydivand and Nikazar, 2015).

3.5 Effect of pH

In order to maximize the effectiveness of this process, it is necessary to determine the optimal operational pH. The pH is an important parameter in the photo-catalyst of TiO_2/ZnO/Fenton process because the pH affects the charge on catalyst particles, size of catalyst aggregates, and the positions of conductance and valence bands (Eydivand and Nikazar, 2015).

Due to the nature of the TiO_2 catalyst used, any variation in the operating pH is known to affect the isoelectric point or the surface charge of the photo-catalyst. Many reports have used the point of zero charge (PZC) of TiO_2 to study the impact of pH on photo-catalytic oxidation performance (Chong *et al.,* 2010).

The PZC is a condition where the surface charge of TiO_2 is zero or neutral and lies in the pH range of 4.5 to 7.0, depending on the catalyst used. At the PZC of TiO_2, the interaction between the photo-catalyst particles and wastewater contaminants is minimal due to the absence of any electrostatic force. When the operating pH is below the pH at PZC (TiO_2), the surface charge for the catalyst becomes positive and gradually exerts an electrostatic attraction force towards the negatively charged compounds. Such polar attractions between TiO_2 and charged anionic carbon compounds can intensify the adsorption onto the photon activated TiO_2 surface for subsequent photo-catalytic reactions (Gogniat *et al.,* 2006). This is particularly significant when the anionic carbon compounds are present at a low concentration level. At operating pH above the pH at PZC (TiO_2), the catalyst surface will be negatively charged and repel the anionic compounds in water (Chong *et al.,* 2010).

Gogate and Pandit, (2004) reported that the influence of initial pH on the photo-catalytic process is more complex and the observed effect is generally dependent on the type of pollutant and the PZC of the photo-catalyst used in the oxidation process. The pH of the medium influences the surface charge properties of the photo-catalyst, and so it has significant effect on the electrostatic interaction between the catalyst surface and the pollutant molecules.

The effect of pH on IC removals by this method was examined with varying pH to treat the petroleum wastewater effluent from SOR with optimum TiO_2 and ZnO dosages, which were 0.3 and 0.58 g L^{-1}, respectively. The results showed that the optimum pH was 7 therefore no need to adjust pH during this treatment and the maximum removal rates of IC were 90.2 as shown in Figure 5.

The maximum degradation of IC from the petroleum wastewater by this method was obtained at pH of 7. The PZC for TiO_2 was determined as pH of 6.28 (Khan *et al.,* 2015; Chou and Liao, 2005; Alaton *et al.,* 2002). The adsorption of anions is favored when pH< $pH_{(zpc)}$. The effects of pH on degradation efficiency in this method were in agreement with findings of other researchers.

The point zero charge of ZnO was reported as pH of 8 (Selvam *et al.,* 2007). The maximum adsorption was observed at pH of 7 for ZnO. The surface of ZnO catalyst is also positively charged. Hence, the maximum degradation occurs, which is in agreement of reported values in literature (Selvam *et al.* 2007).

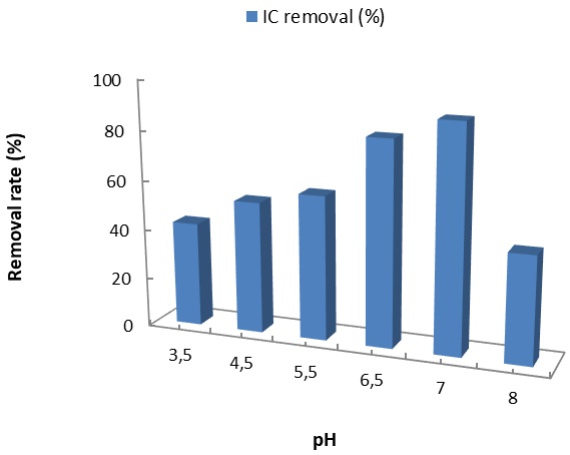

Figure 5. Influence of the initial pH on the degradation rate of IC by the solar photo-catalyst of TiO_2/ZnO/Fenton process

4. Conclusion

The performance of solar photo-catalyst of TiO_2 process was significantly improved by adding of ZnO/Fenton to it during the solar photo-catalyst TiO_2/ZnO/Fenton process at the neutral value of pH to treat the petroleum wastewater from 15% to 90.2% for IC removal. So, the TiO_2/ZnO/Fenton/solar is a good choice application in IC removal from the petroleum wastewater from SOR. Not only because it can achieve 90.2% of IC removals, but also because the process is cost-effective and simple in a technological aspect. Furthermore, the catalysts (TiO_2 and ZnO) are non-toxic and the effluent is almost neutral (pH 7), therefore, no there is need to adjust pH during this treatment. The quadratic models proved to be significant with very low probabilities (<0.0001) for the IC removal and residual iron. The optimum conditions for the solar photo-catalyst of TiO_2/ZnO/Fenton were a TiO_2 dosage (0.3 g/l), ZnO dosage (0.58 g/l), Fe^{+2} dosage (0.02 g/l), H_2O_2 dosage (2.7 g/l), and pH (7). The maximum removal rate for IC and residual iron was 92.3% and 0.013, respectively. The treatment process achieved higher degradation efficiencies for IC and reduced the treatment time comparing with other related processes.

References

Abu Amr S.S., Hamidi A.A., Mohd N.A. and Mohammed J.K. (2013), Optimization of semi-aerobic stabilized leachate treatment using ozone/Fenton's reagent in the advanced oxidation process, *Journal of Environmental Science and Health Part A*, **48**, 720-729.

Adesina A.A. (2004), Industrial exploitation of photocatalysis: progress, perspectives and prospects, *Catalysis Surveys from Asia*, **8**(4), 265-273.

Ahmad A.L., Ismail S. and Bhatia S. (2005), Optimization of coagulation-flocculation process for palm oil mill effluent using response surface methodology, *Environ. Sci. Technol.,* **39**, 2828-2834.

Ahmed S., Rasul M.G., Martens W.N., Brown R. and Hashib M.A. (2010), Heterogeneous photocatalytic degradation of phenols in wastewater: a review on current status and developments, *Desalination*, **261**, 3-18.

Akpan U.G. and Hameed B.H. (2009), Parameters affecting the photocatalytic degradation of dyes using TiO_2-based photocatalysts: a review, *J. Hazard. Mater.*, **170**, 520-529.

Alaton I.A., Balcioglu I.A. and Bahnemann D.W. (2002), Advanced oxidation of a reactive dyebath effluent: comparison of O_3, H_2O_2/UV-C and TiO_2/UV-A processes, *Water Research*, **36**, 1143-1154.

Al Jabri H. and Feroz S. (2015), The Effect of Combining TiO_2 and ZnO in the Pretreatment of Seawater Reverse Osmosis Process, *International Journal of Environmental Science and Development*, **6**(5), 348-351.

Aljuboury D.D.A., Palaniandy P., Abdul Aziz H.B. and Feroz S. (2015), Treatment of petroleum wastewater using combination of solar photo-two catalyst TiO_2 and photo-Fenton process, *Journal of Environmental Chemical Engineering*, **3**, 1117-1124.

Alhakimi G., Studnicki L.H. and Al-Ghazali M. (2003), Comparative photocatalytic degradation using natural and artificial UV-light of 4-chlorophenol as a representative compound in refinery wastewater, *Journal of Photochemistry and Photobiology A: Chemistry*, **157**, 103-109.

Al-Rasheed R.A. (2005), Water treatment by heterogeneous photocatalysis an overview. 4th SWCC Acquired Experience Symposium held in Jedda. 1-14.

Barick K.C., Sharma P., Mukhija A., Sainis J.K., Gupta A. and Hassan P.A. (2015), Effect of cetylpyridinium chloride on surface passivation and photocatalytic activity of ZnO nanostructures, *J. Environ. Chem. Eng.*, **3**(2), 1346–1355.

Bickley R.I., Slater M.J. and Wang W.J. (2005), Engineering development of a photcatalytic reactor for wastewater treatment, *Process Safe. Environ. Protect.*, **83**, 205-216.

Chakrabarti S. and Dutta B. (2004), Photocatalytic degradation of model textile dyes in wastewater using ZnO as semiconductor catalyst, *J. Hazard Mater.*, **112**, 269-278.

Cheng C., Amini A., Zhu C., Xu Z., Song H. and Wang N. (2014), Enhanced photocatalytic performance of TiO_2-ZnO hybrid nanostructures, *Scientific Reports*, **4**, 4181.

Chou J.C. and Liao L.P. (2005), Study on pH at the point of zero charge of TiO_2 pH ion sensitive field effect transistor made by the sputtering method, *Thin Solid Films*, **476**, 157-161.

Chong M.N., Jin B., Chow C.W.K. and Saint C. (2010), Recent developments in photocatalytic water treatment technology: A review, *Water Research*, **44**, 2997-3027.

De Morais J.L. and Zamora P.P. (2005), Use of advanced oxidation processes to improve the biodegradability of mature landfill leachates, *J. Hazard. Mater.*, **123**, 181-186.

Ehrampoush M.H., Moussavi G.H.R., Ghaneian M.T., Rahimi S. and Ahmadian M. (2011), Removal of methylene blue dye from textile simulated sample using tubular reactor and TiO2/UV-C photocatalytic process, *Iran. J. Environ. Health. Sci. Eng.*, **8**, 35-40.

El-Gendy N.S., Madian H.R. and Abu Amr S.S. (2013), Design and optimization of a process for sugarcane molasses fermentation by saccharomyces cerevisiae using response surface methodology, *Int. J. Microbiology*, **1**, 1–9.

Eydivand S. and Nikazar M. (2015), Degradation of 1,2-Dichloroethane in simulated wastewater solution: A comprehensive study by photocatalysis using TiO_2 and ZnO nanoparticles, *Chem. Eng. Communicat.*, **202**, 102-111.

Gaya U.I. and Abdullah A. (2008), Heterogeneous photocatalytic degradation of organic contaminants over titanium dioxide: a review of fundamentals, progress and problems, *Journal of Photochemistry and Photobiology C: Photochemistry Reviews,* **9**, 1-12.

Gogate P.R. and Pandit A.B. (2004), A review of imperative technologies for wastewater treatment I: oxidation technologies at ambient conditions, *Adv. Environ. Res.*, **8**, 501-551.

Gogniat G., Thyssen M., Denis M., Pulgarin C. and Dukan S. (2006), The bactericidal effect of TiO2 photocatalysis involves adsorption onto catalyst and the loss of membrane integrity, *FEMS Microbiol. Letter*, **258**, 18-24.

Heredia J.B.D., Torregrosa J., Dominguez J.R. and Peres J.A. (2001), Oxidation of p-hydroxybenzoic acid by UV radiation and by TiO_2/UV radiation: comparison and modeling of reaction kinetic, *J. Hazard. Mater.*, **83**, 255.

Khan W.Z., Najeeb I., Tuiyebayeva M. and Makhtayev Z. (2015), Refinery wastewater degradation with titanium dioxide, zinc oxide, and hydrogen peroxide in a photocatalytic reactor, *Process Safety and Environmental Protection*, **9**, 479-486.

Kim J.L., Lee H. and Lee C. (2012), Synergistic effects of TiO_2 photocatalysis in combi-nation with Fenton-like reactions on oxidation of organic compounds at circumneutral pH, *Applied Catalysis B: Environmental*, **115**, 219-224.

Konstantinou I.K. and Albanis T.A. (2004), TiO_2-Assisted photocatalytic degradation of Azo dyes in aqueous solution: Kinetic and Mechanistic Investigations: A review, *Appl. Catal. B: Environ.*, **49**, 1–14.

Mathur A., Raghavan A., Chaudhury P., Johnson J.B., Roy R., Kumari J., Chaudhuri G., Chandrasekaran N., Suraishkumar G.K. and Mukherjee A. (2015), Cytotoxicity of titania nanoparticles towards waste water isolate Exiguobacterium acetylicum under UVA, visible light and dark conditions, *J. Environ. Chem. Eng.*, **3**(2), 1837–1846.

Mehrotra K., Yablonsky G.S. and Ray A.K. (2003), Kinetic studies of photocatalytic degradation in a TiO_2 slurry system: distinguishing working regimes and determining rate dependences, *Ind. Eng. Chem. Res.*, **42**, 2273.

Mohajeri S., Hamidi A.A., Isa M.H., Bashir M.J.K. and Mohajeri L. (2010), Influence of Fenton reagent oxidation on mineralization and decolorization of municipal landfill leachate, *J. Environ. Sci. Heal. A*, **45**, 692–698.

Montgomery D.C. (2008) Design and Analysis of Experiments. 7th edition.

Noordin V.C., Venkatesh S., Sharif S. and Elting A.A. (2004), Application of response surface methodology in describing the performance of coated carbide tools when turning AISI 1045 steel, *Journal of Materials Processing Technology*, **145**, 46-58.

Selvam K., Muruganandham M., Muthuvel I. and Swaminathan M. (2007), The influence of inorganic oxidants and metal ions semiconductor sensitized photo-degradation of 4-fluorophenol, *Chem. Eng. J.*, **128**, 51-57.

Sobczyński A. and Dobosz A. (2001), Water Purification by Photocatalysis on Semiconductors, *Polish Journal of Environmental Studies*, **10**(4), 195-205.

Tony M.A., Zhao Y.Q., Purcell P.J. and El-Sherbiny M.F. (2009), Evaluating the photo-catalytic application of Fenton's reagent augmented with TiO_2 and ZnO for the mineralization of an oil-water emulsion, *Journal of Environmental Science and Health*, *Part A*, **44**, 488-493.